

Benchmarks for model validation based on lidar wake measurements

P Doubrawa¹, M Debnath¹, P J Moriarty¹, E Branlard¹,
T G Herges², D C Maniaci², B Naughton²

¹National Renewable Energy Laboratory, Golden, CO, USA

²Sandia National Laboratories, Albuquerque, NM, USA

E-mail: Paula.Doubrawa@nrel.gov

Abstract. Technology development and design decisions in wind energy are often based on results from simulations performed for individual wind turbines or entire wind plants. It is therefore critical to ensure that the models being used for research and industry applications in wind energy be thoroughly validated against measurements. A full-system validation of wind plant simulations must consider the atmospheric inflow, the response of the wind turbines, and their wakes. This task is complicated by the lack of freely available, quality-controlled, high-quality measurements. Here, such measurements are used to offer a validation exercise that can be used to assess the accuracy of models of any fidelity level. When it comes to real-world measurements, the dataset considered herein is simple in terms of terrain but exhibits pronounced diurnal cycles. Instead of a full-scale wind plant, we consider an individual research-scale, utility wind turbine instrumented for power and loads measurements. Three benchmarks are defined, with increasing levels of complexity: near neutral, slightly unstable, and very stable atmospheric stratification. Through comparisons between observations and simulations, the benchmarks provide complementary information about the model performance and its ability to reproduce mean and dynamic wake characteristics. This article describes the measurements and methodology used to define these benchmarks and provides the information required to perform simulations and conduct the model-measurement comparison. The objective is to provide a robust wake model validation exercise open to anyone, which will serve to minimize uncertainty in model validation practices related to varying methodologies across simulation tools and users.

1. Introduction

Atmospheric stratification has a large impact on wind-plant performance [1, 2] and reliability [3]. This impact becomes increasingly important as new technology continuously pushes the boundaries of wind-turbine rotor sizes and extends the footprint of wind plants. As a result, the application scope of wind-turbine wake models is continuously broadened as they are used to simulate progressively larger systems and more complex environmental conditions. As these models are pushed to their limits or further developed to higher fidelity levels, it is necessary to continuously ensure that the research and industry communities can rely on them for the development of new and improved technology.

The impact of wind turbine wakes on power production has been studied extensively, both from the perspective of wind plant measurements [4] and wind plant simulations [5]. Validation studies focusing on power have been performed for models ranging across fidelity levels: from simple analytical models [6] to large-eddy simulation codes [7]. However, model validation



considering turbine loads and wake measurements are rare. While several field measurements of wind turbine wakes have been performed (i.e., at least 12 datasets have been collected [8]), few studies (e.g., [9]) have considered them in wake model validation exercises.

Based on this limited body of work, there is a clear need for more opportunities for wake model validation. To address this need, we propose herein three wake model validation benchmarks that can be applied to any wind-turbine wake model. The validation focuses on quality-controlled, high-resolution measurements of a single wake performed with a rear-facing scanning lidar (Figure 1) mounted on the nacelle of a modified V27 wind turbine at the Scaled Wind Farm Technology (SWiFT) facility in Lubbock, Texas, USA [10]. This heavily instrumented site in the U.S. Great Plains provides the opportunity to validate simulations of wind-turbine wakes without the influence of complex terrain or larger scale meteorological forcings, and therefore allows us to focus entirely on atmospheric stratification effects.

The benchmarks defined herein are unique in terms of the quality and quantity of data used to define them. Each of the three benchmarks is defined based on measurements of the inflow, the wind turbine, and the wake. The objective of this work is to provide a thorough description of these benchmarks and the methodology used to define them. This paper can serve as a reference for any modelers interested in a standardized validation exercise that offers the possibility of validating the full system (atmosphere, turbine, and wake) while still maintaining relative simplicity (a single wake at a site with flat terrain).



Figure 1: Schematic of SWiFT facility showing the three V27 wind turbines, the meteorological towers located south of the wind turbines, and one of the DTU SpinnerLidar scanning strategies employed for the SWiFT benchmarks (scanning towards the north).

2. Measurements used to define the benchmarks

2.1. Available Measurements

2.1.1. Inflow The inflow conditions to the 27-m rotor diameter wind turbine are approximated from atmospheric measurements collected with a 60-meter meteorological tower located approximately 2.5 rotor diameters (D) due south (the predominant wind direction) of the wind turbine location (the turbine and tower to the east in Fig. 1). The wind measurements are obtained with five sonic anemometers, three cup anemometers, and one wind vane. Two pressure sensors, three temperature sensors, and three humidity sensors are also available between 2.5 m and 56.5 m above ground ($z_{hub} = 32.1$ m) and used to diagnose the atmospheric state at the site [10].

2.1.2. Wind turbine The wind turbine considered in the SWiFT benchmarks is a variable-speed, variable-pitch, modified and instrumented Vestas V27. While there are three wind turbines at the site, only one was equipped with a nacelle-mounted lidar to measure its wake and is used to define the benchmarks (the southeastern turbine in Fig. 1). In addition to rotor speed and generator power and torque, strain sensors at the blade root were used to estimate the flapwise bending moment of one blade.

An aeroelastic model of this turbine was developed for the OpenFAST simulation tool [11] and calibrated against measurements [12] and is publicly available [13]. Section 2.1.2 shows the turbine power curve for all measurements used to define each benchmark and for the OpenFAST

turbine model. The triangles mark the ensemble mean hub-height wind speed values provided to the modelers and the ensemble mean power to be used when validating turbine operation statistics. The large scatter in the observed power curve highlights one of the main challenges in validating idealized simulations against real-world measurements: prescribing the initial and boundary conditions to the simulation so that the fluctuations in the turbine response will be adequately captured. As described in Section 4, we propose to address this challenge by introducing a model calibration step prior to the wake validation step.

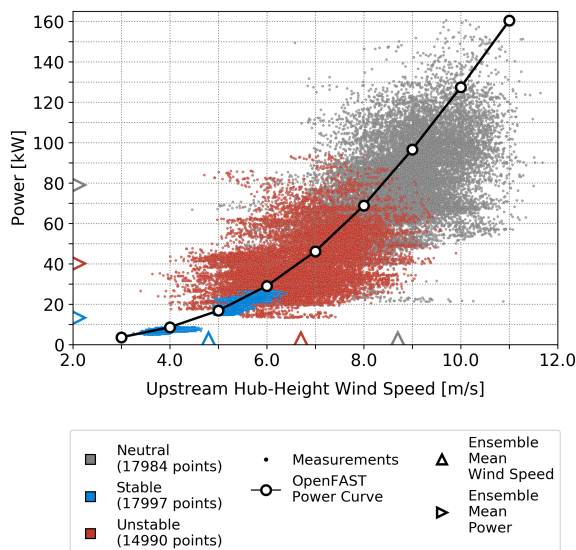


Figure 2: Generator power vs. hub-height wind speed for measurements (dots) for the OpenFAST simulations (line). Ensemble mean hub-height wind speed and power are given (triangles).

2.1.3. Wake The wake measurements were obtained with a rear-facing, nacelle-mounted DTU SpinnerLidar [14]. The lidar sampling was configured differently depending on the motivation behind each experiment: measuring at a single distance downstream, but at higher temporal frequency (i.e., every ~ 2 s) when seeking to characterize the dynamic behavior of the wake; or sampling up to 7 distances downstream (as shown in Fig. 1) at lower temporal frequency (i.e., every $\sim 30 - 42$ s) when focusing on the spatial evolution of the mean wake along the downstream direction. The maximum focus distance of the beams is ~ 135 m, which is approximately 5 D for the V27 rotor. The distance between the two turbines which are aligned in the south-north direction is also 5 D, and therefore the downstream turbine was shutdown when collecting wake measurements for these benchmarks. While measurements are available as close to the rotor as 1 D, the wake is not clearly defined at this distance and therefore only measurements starting at 2 D are used for the model validation.

2.2. Sub-sampling

of available measurements for the benchmarks

To define the three benchmarks, periods with large offsets between nacelle position and wind direction were first filtered out. The remaining data were divided into 10-minute periods for which statistics of the inflow were computed. These 10-minute periods were clustered based on how similar they were in terms of the wake measurement strategy (i.e., number of downstream distances measured) and the upstream flow characteristics. The atmospheric quantities considered in this clustering were U_{hub} , TI_{hub} , α , and z/L (see glossary for variable definitions).

These clusters of 10-minute periods were then further analyzed (with synoptic charts and meteorological data from surface stations) to ensure that no large-scale meteorological forcings (e.g., fronts bringing wind direction or air temperature changes) were present, which would complicate the simulation setup. Clusters of 10-minute periods free of synoptic forcing were then ensemble averaged to define the benchmarks.

2.3. Processing of wake measurements for validation

First of all, the lidar measurements undergo basic quality control (e.g., based on hard target detection and signal-to-noise ratio of the retrievals). Then, the lidar-derived line-of-sight velocity (v_{los}) is interpolated (using natural-neighbor interpolation) from the rosette pattern of the scan (Fig. 1) onto a two-dimensional regular grid spanning the lateral and vertical directions.

Once the v_{los} field is interpolated onto a regular grid, the wake edge and center are approximated in each scan (a “scan” refers to a set of points sampled by the lidar over a period of ~ 2 s at a given distance downstream). First, the velocity deficit is calculated by subtracting the vertical profile of the inflow (estimated from the meteorological mast measurements) from the wake velocity values (note that for the data presented here, this deficit is also normalized by the inflow). Then, the wake edge is identified as the velocity deficit contour that matches a pre-specified area that the algorithm seeks to match when tracing this contour. Finally, the wake center is identified as the centroid of the velocity deficit field within the wake edge. Several other methods exist to identify the wake edge and center, and other possibilities will be explored in future work.

For the wake measurements shown here, each scan is translated so that its coordinate system origin is at the wake center. Then, temporal averages are obtained in this meandering frame of reference (MFoR) for each 10-minute period used to define the benchmarks. Finally, an ensemble mean is obtained by averaging these temporally averaged wakes across the 5 or 6 datasets used to define each benchmark.

3. The SWiFT benchmarks

3.1. Benchmark for a near-neutral atmosphere

Hereinafter, the term “evolution” refers to the spatial evolution of the wake as it propagates and dissipates downstream. The model-measurement comparison focus is on temporally averaged quantities which are diagnosed from wake measurements collected at low temporal frequency (i.e., every $\sim 30 - 42$ s). This case is the most straight-forward benchmark case, as it assumes no atmospheric stratification effects.

Six 10-minute periods with near-neutral conditions and similar wind speed and turbulence intensity were selected to define this benchmark. The 10-minute statistics of each period are given in Table 1, along with the mean of these periods (i.e., the “ensemble” mean), which are provided to drive the simulations. For context within the diurnal radiative cycle, we provide the time offset between the beginning of the selected 10-minute period and the sunrise or sunset for that day. For this neutral case, most periods are within 1.5 hours of either sunrise or sunset, indicating an environment that is likely within the transition period between the nighttime stable boundary layer and daytime convective conditions.

Even for the neutral case, which is the simplest of the benchmarks, the mean change in wind direction with height (i.e., veer) can be different depending on the 10-minute period considered (Fig. 3a). However, rotor veer was not provided to the participants as a constraining parameter to drive the simulations. In this paper, it is provided to present a broader picture of the atmospheric conditions and to support the interpretation of results when model and measurement data are compared.

The SWiFT measurements were collected during a wake steering campaign that took place between 2016 and 2017. However, the benchmarks focus on aligned conditions, i.e. the turbine being simulated is fully aligned with the mean inflow. Therefore, the measurement periods selected for this benchmark have yaw offset values as close to zero as possible. For the neutral and unstable benchmarks (see Fig. 4), the mean yaw offset is close to zero but fluctuations in the wind direction lead to a high variance in this quantity (the non-zero mean yaw offset of the stable case will be discussed in Section 3.3). To start off with a simpler validation exercise, no yaw offset values were provided to participants of the benchmarks. Results of the measurement-model

Table 1: Atmospheric conditions for each 10-minute period used to define the neutral stratification benchmark, and the ensemble mean used to constrain the simulations. Variable symbols are given in the glossary.

Time from Sunrise or Sunset (h)	U_{hub} (m/s)	σ_u (m/s)	σ_v (m/s)	σ_w (m/s)	TI_{hub} (%)	α (-)	z/L (-)	u_* (m/s)	$\overline{w'\theta'_v}$ (K m/s)	θ_v (K)
Sunset-1.3	8.2	1.05	1.01	0.62	12.7	0.13	-0.010	0.51	0.011	305.8
Sunset-0.7	9.0	1.04	0.64	0.46	11.6	0.11	0.002	0.50	-0.002	318.8
Sunset-0.5	8.6	0.83	0.74	0.47	9.6	0.13	0.019	0.42	-0.012	318.3
Sunset-0.4	8.5	0.98	0.67	0.47	11.4	0.17	0.032	0.42	-0.019	317.8
Sunset-0.2	8.8	0.87	0.71	0.47	9.9	0.17	0.031	0.44	-0.022	317.5
Sunrise+2.3	9.1	0.85	0.83	0.54	9.4	0.13	-0.048	0.43	0.029	308.4
Ensemble Mean	8.7	0.93	0.77	0.50	10.7	0.14	0.004	0.45	-0.002	314.4

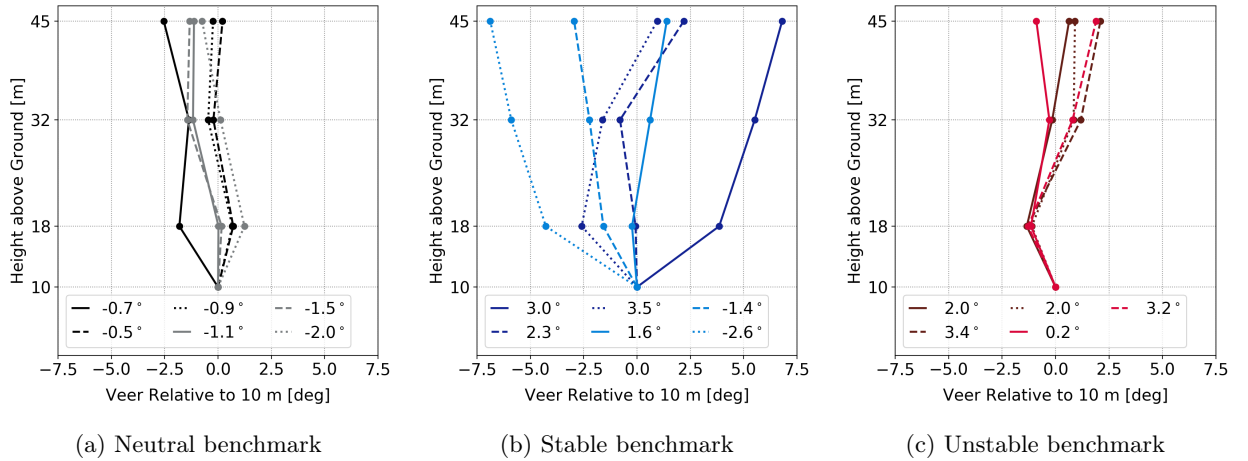


Figure 3: Mean wind direction change with height (positive values refer to wind veering and negative values to wind backing) for each 10-minute period (lines) used to define each of the three benchmarks. Values in the legend give mean veer across the rotor (i.e., difference in wind direction between 45 m and 18 m).

comparison will indicate whether perturbations in wind direction or in the yaw response of the turbine are necessary to validate simulations that use ideal inflow conditions against real-world data.

Fig. 5 shows the velocity deficit ensemble mean considering all scans used to define the neutral benchmark. The wake is given in a meandering frame of reference, meaning that the origin of the coordinate system moves in time (as it follows the wake center) with respect to the fixed frame of reference of the turbine. The measurements clearly indicate an expansion and recovery of the wake between 2 D and 5 D, and reveal a radially symmetric wake. A more quantitative analysis can be obtained from Fig. 6a, which indicates a recovery from 60% to almost 40% in the maximum deficit of the mean wake.

3.2. Benchmark for a slightly unstable atmosphere

Rather than focusing on the spatial evolution of mean quantities, the validation exercise under the unstable benchmark focuses on the dynamic behavior of the wake at discrete distances downstream. For this case, the lidar was measuring the wake at a single downstream distance. Therefore the sampling frequency is higher (i.e., every ~ 2 s) and allows for an analysis that

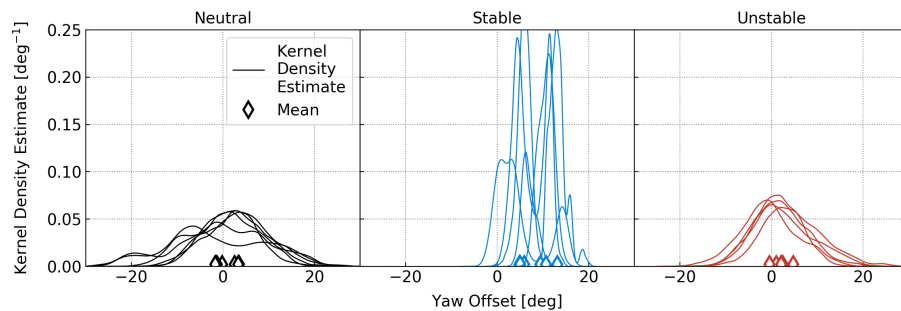


Figure 4: Probability density function (evaluated as a kernel density fit) for the time series of yaw offset (difference between incoming wind direction and nacelle yaw position) for each 10-minute period (lines) used to define each benchmark. Diamonds mark the mean yaw offset for each of the curves.

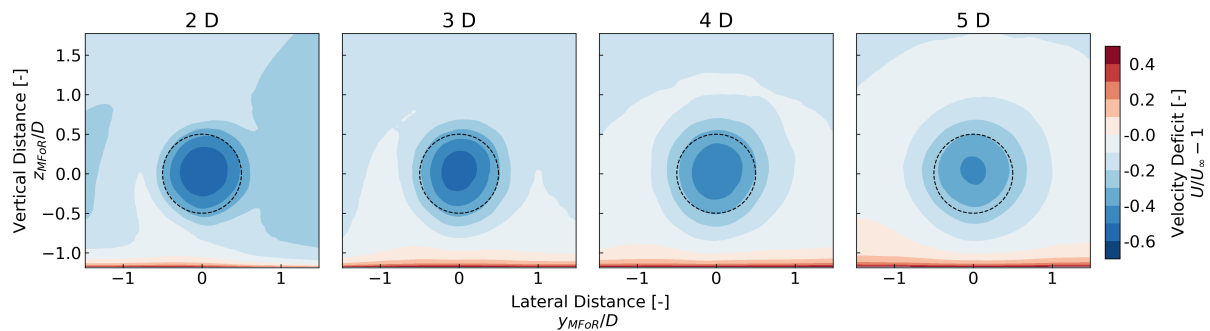


Figure 5: Mean wake from lidar measurements for the neutral benchmark. Planes are in a meandering frame of reference (MFoR). Dashed black line marks the rotor outline.

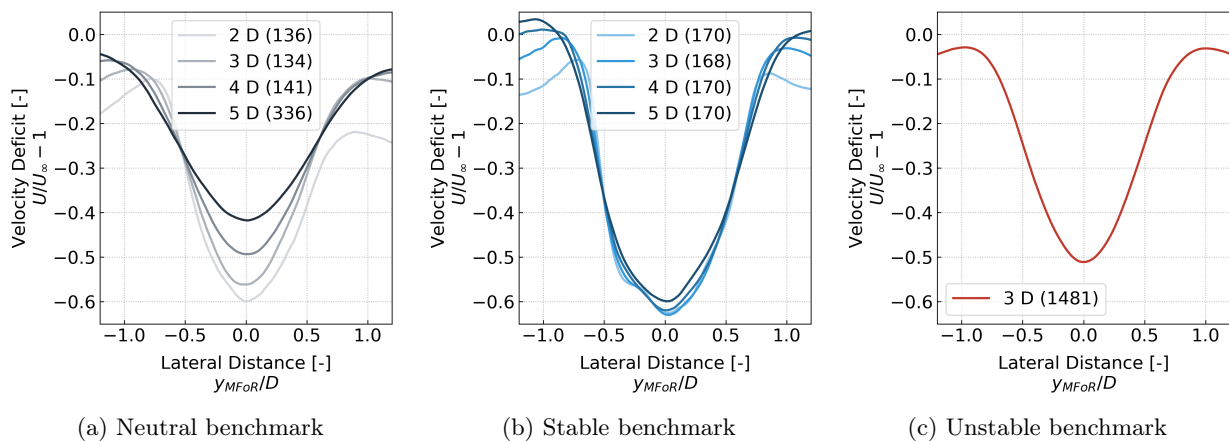


Figure 6: Lateral profiles of velocity deficit at hub height as diagnosed from lidar measurements. Lateral coordinate is in a meandering frame of reference (MFoR). Numbers in parentheses indicate how many scans were averaged to obtain the mean profiles. Values beyond $y/D \pm 0.5$ are more uncertain, as they may move in and out of the lidar field of view as the wake moves.

considers unsteady phenomena driven by turbulence, such as wake meandering.

While the lidar sampling strategy here differs substantially from the one in the neutral benchmark, the mean atmospheric conditions are not too different as can be seen in Table 2. The

Table 2: Similar to Table 1 but for the unstable stratification benchmark.

Time from Sunrise (h)	U_{hub} (m/s)	σ_u (m/s)	σ_v (m/s)	σ_w (m/s)	TI_{hub} (%)	α (-)	z/L (-)	u_* (m/s)	$\overline{w'\theta'_v}$ (K m/s)	θ_v (K)
+1.2	6.8	0.81	0.60	0.46	11.9	0.20	-0.038	0.37	0.015	289.4
+1.3	6.1	0.72	0.58	0.42	11.8	0.14	-0.132	0.23	0.013	290.0
+1.5	6.3	0.89	0.70	0.52	14.0	0.13	-0.077	0.34	0.022	290.7
+1.7	6.6	0.97	0.62	0.52	14.6	0.14	-0.074	0.36	0.026	291.4
+2.0	7.4	0.80	0.72	0.53	10.6	0.09	-0.126	0.35	0.040	293.0
Ensemble Mean	6.7	0.84	0.65	0.49	12.6	0.14	-0.089	0.33	0.023	290.9

inflow has lower wind speeds and higher turbulence, but the wind shear values are similar. The main difference is in the mean stability parameter, which clearly indicates unstable rather than neutral stratification. Another difference is the veering of wind with height (Fig. 3c), in contrast to the backing seen for the neutral case (Fig. 3a). Simulations of the neutral and unstable benchmarks are expected to provide more insight as to how flow structures differ between the two scenarios, and how these affect the wind turbine response. This small increase in simulation complexity level from the neutral to the unstable case allows for a building-block approach to model validation, building confidence in the simulation tool before the more difficult stable case is tackled.

The mean wake as measured by the lidar is shown in Fig. 7. Note that for this benchmark, measurements were only collected at $x = 3$ D. At this distance, the radially symmetric unstable wake has recovered slightly more than the neutral wake as can be quantified by comparing the maximum deficit values between Fig. 6c ($\sim 51\%$) and Fig. 6a ($\sim 56\%$).

3.3. Benchmark for a very stable atmosphere

Similarly to the neutral benchmark, the stable benchmark also focuses on the spatial evolution of the wake along its downstream propagation. Remote sensing measurements of the wake are available for these periods at 7 distances downstream of the rotor, but only the distances 2, 3, 4, and 5 D are considered here. In defining this benchmark, there were no measurement periods available with similar inflow and lidar measurement strategy, and zero-mean yaw offset. Therefore, the relatively large yaw offsets in this benchmark (Fig. 4) were unavoidable, as the periods used to define it were the only stable ones during which wind speed, turbulence intensity, and shear were similar. While this yaw offset may reveal a challenge in the model validation exercise, the very stable atmospheric conditions make for a well-defined wake which is easier to measure and characterize.

The inflow conditions here (Table 3) are extremely different than the previous— low wind speed,

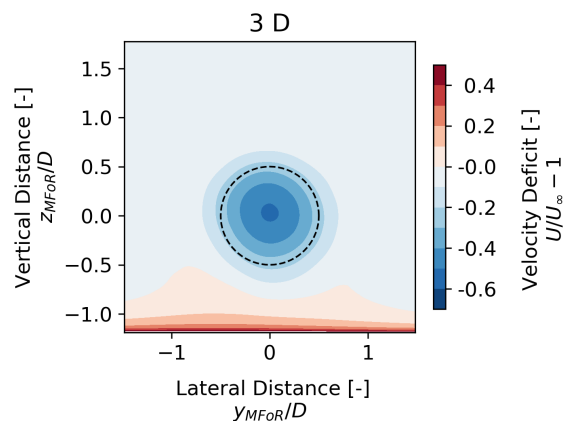


Figure 7: Mean wake from lidar measurements for the unstable benchmark. Planes are in a meandering frame of reference (MFoR). Dashed black line marks the rotor outline.

low turbulence intensity, and high shear make this a unique and challenging case to simulate. This very stable benchmark was defined with the intent of pushing models to their limits. Models are expected to differ the most for this benchmark, and therefore the most value can be gained here in terms of identifying weaknesses in our modeling strategies which need to be addressed so we can simulate wider ranges of stratification conditions for wind energy applications.

Table 3: Similar to Table 1 but for the stable stratification benchmark.

Time from Sunset (h)	U_{hub} (m/s)	σ_u (m/s)	σ_v (m/s)	σ_w (m/s)	TI_{hub} (%)	α (-)	z/L (-)	u_* (m/s)	$\overline{w'\theta'_v}$ (K m/s)	θ_v (K)
+5.3	4.2	0.13	0.17	0.07	3.1	0.44	1.438	0.05	-0.001	303.7
+5.5	4.1	0.14	0.11	0.07	3.5	0.49	0.822	0.05	-0.001	303.6
+5.7	3.9	0.18	0.19	0.06	4.6	0.56	0.978	0.08	-0.003	303.6
+6.2	5.3	0.15	0.21	0.03	3.0	0.49	0.963	0.09	-0.005	305.0
+6.3	5.3	0.14	0.11	0.05	2.6	0.48	1.903	0.07	-0.005	304.8
+6.5	5.7	0.21	0.18	0.09	3.7	0.56	0.799	0.13	-0.014	304.6
Ensemble Mean	4.8	0.16	0.16	0.06	3.4	0.50	1.151	0.08	-0.005	304.2

The wake under stable conditions (Fig. 8) shows more asymmetry in the velocity distribution field than the wakes for the neutral and unstable benchmarks. Due to the very low turbulence, the stable wake also does not recover or expand much as it propagates downstream. In fact, the maximum deficit shows little recovery between 2 D and 4 D: $\sim 3\%$ (compare to $\sim 18\%$ for the neutral benchmark).

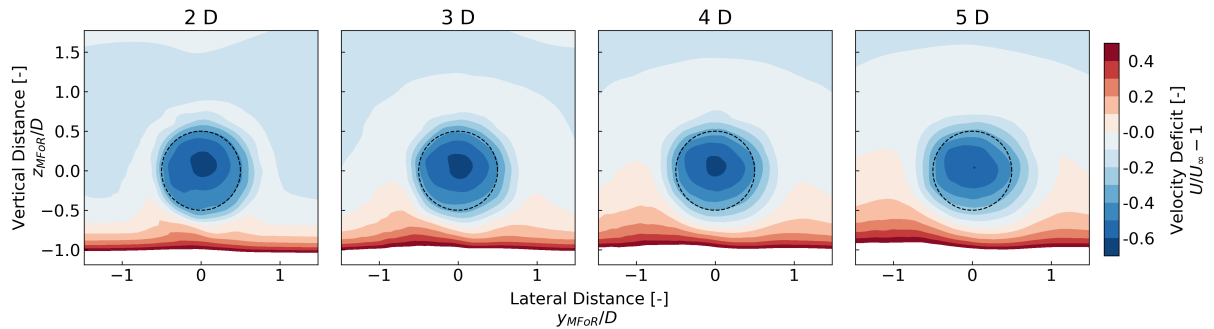


Figure 8: Mean wake from lidar measurements for the stable benchmark. Planes are in a meandering frame of reference (MFoR). Dashed black line marks the rotor outline.

4. Proposed simulation strategy

To simulate these benchmarks, modelers should use the ensemble mean values provided in Tables 1 to 3 to drive their atmospheric inflow simulations. The wake model validation exercise proposed herein is composed of a model calibration step followed by a model improvement step, as shown by the schematic in Fig. 9. First, the provided inflow values and turbine model are used to drive atmospheric inflow and wind turbine simulations which are repeated until the simulated inflow and wind turbine response match the measured signals to the desired level. The “desired level” will vary depending on the level of fidelity of the model and the simulated time, so that the model solution is sufficiently converged and therefore appropriate for validation. Once the

modeled turbine responds as expected, the actual wake simulation is performed and compared to wake measurements. Here, we suggest including a model of the lidar in the simulation, as an added level of wake-focused validation (details about the implementation of a lidar model are beyond the scope of this paper, but relevant information can be found in [15]). The results of this comparison serve to inform the modeler on the shortcomings of the model or the simulation tool being used. At this point, the model can be improved and the wake simulation and validation step can be repeated as needed until the model limitations have been addressed and the validation results are satisfactory.

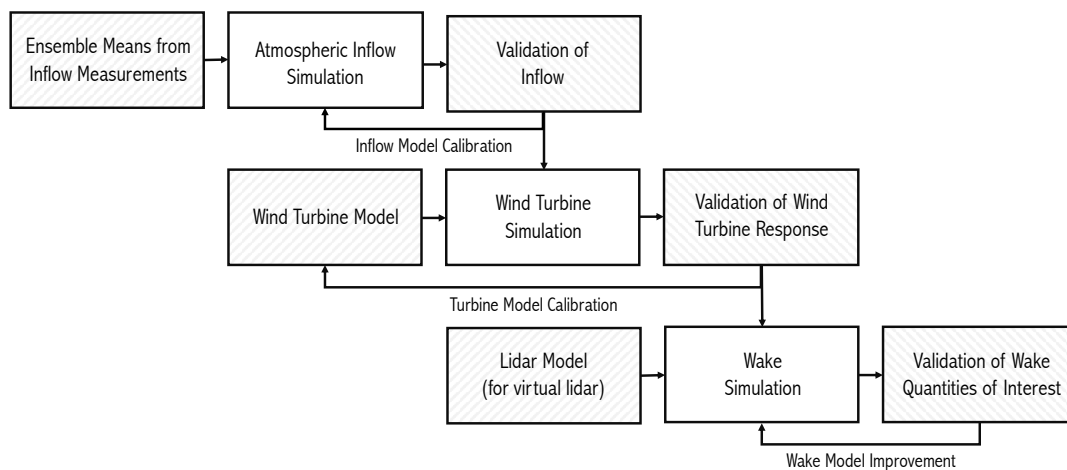


Figure 9: Schematic of proposed approach for wake model validation.

5. Summary

This paper presented three benchmarks that can be used to validate wake models of varying fidelity levels. These benchmarks consider the full-system (atmosphere, turbine, and wake) while still maintaining relative simplicity (a single wake in an atmospheric environment free of synoptic forcing and on simple terrain). The three benchmarks represent building blocks for model validation: first, a simple scenario where neutral stratification can be assumed. Next, some complexity is added and a slightly unstable case is defined followed by a challenging, very stable scenario. When combined, these can be used to identify shortcomings in model performance and drive model development directions.

In the future, all measurements will be freely available [16] and modelers across the community are encouraged to use the data presented here to validate their wake models according to the simulation guidelines proposed. A future publication will describe in detail the quantities of interest and validation metrics used for the wake validation exercise, along with validation results considering models of various fidelity levels: from steady-state analytical models to large-eddy simulations. Together, the current and future publications will provide a standardized validation framework for the SWiFT Benchmarks and a blueprint for future benchmarking exercises. This standardization seeks to reduce uncertainty due to varying validation approaches and ensure consistent results across the wake modeling community.

6. References

- [1] Clara M. St Martin, Julie K. Lundquist, Andrew Clifton, Gregory S. Poulos, and Scott J. Schreck. Wind turbine power production and annual energy production depend on atmospheric stability and turbulence. *Wind Energy Science*, 1(2):221–236, November 2016.

- [2] Said El-Asha, Lu Zhan, and Giacomo Valerio Iungo. Quantification of power losses due to wind turbine wake interactions through SCADA, meteorological and wind LiDAR data. *Wind Energy*, 20(11):1823–1839, 2017.
- [3] M. C. Holtslag, W. a. a. M. Bierbooms, and G. J. W. van Bussel. Wind turbine fatigue loads as a function of atmospheric conditions offshore. *Wind Energy*, 19(10):1917–1932, 2016.
- [4] Kurt S. Hansen, Rebecca J. Barthelmie, Leo E. Jensen, and Anders Sommer. The impact of turbulence intensity and atmospheric stability on power deficits due to wind turbine wakes at Horns Rev wind farm. *Wind Energ.*, 15(1):183–196, January 2012.
- [5] Cristina L. Archer, Sina Mirzaeisfat, and Sang Lee. Quantifying the sensitivity of wind farm performance to array layout options using large-eddy simulation. *Geophysical Research Letters*, 40(18):4963–4970, 2013.
- [6] R. J. Barthelmie, S. C. Pryor, S. T. Frandsen, K. S. Hansen, J. G. Schepers, K. Rados, W. Schlez, A. Neubert, L. E. Jensen, and S. Neckelmann. Quantifying the Impact of Wind Turbine Wakes on Power Output at Offshore Wind Farms. *J. Atmos. Oceanic Technol.*, 27(8):1302–1317, February 2010.
- [7] Yu-Ting Wu and Fernando Porté-Agel. Modeling turbine wakes and power losses within a wind farm using LES: An application to the Horns Rev offshore wind farm. *Renewable Energy*, 75:945–955, March 2015.
- [8] Simon-Philippe Breton, J. Sumner, Jens Nørkær Sørensen, Kurt Schaldemose Hansen, Sasan Sarmast, and S. Ivanell. A survey of modelling methods for high-fidelity wind farm simulations using large eddy simulation. *Philosophical Transactions of the Royal Society A: Mathematical, Physical and Engineering Sciences*, 375(2091), 2017.
- [9] E. Machefaux, G. C. Larsen, N. Troldborg, Kurt S. Hansen, N. Angelou, T. Mikkelsen, and J. Mann. Investigation of wake interaction using full-scale lidar measurements and large eddy simulation. *Wind Energy*, 19(8):1535–1551, 2016.
- [10] Christopher Lee Kelley and Brandon Lee Ennis. SWiFT site atmospheric characterization. Technical Report SAND2016-0216, Sandia National Laboratories (SNL-NM), Albuquerque, NM (United States), 2016.
- [11] NREL. OpenFAST repository, 2019. <https://github.com/OpenFAST/openfast>.
- [12] Christopher Lee Kelley and Jonathan White. An Update to the SWiFT V27 Reference Model. Technical Report SAND2018-11893, Sandia National Laboratories (SNL-NM), Albuquerque, NM (United States), 2018.
- [13] NREL. The SWiFT Benchmarks GitHub Repository, 2019. https://github.com/NREL/wakebench_swift.
- [14] Torben Mikkelsen, Nikolas Angelou, Kasper Hjorth Hansen, Mikael Sjöholm, M. Harris, C. Slinger, P. Hadley, R. Scullion, G. Ellis, and G. Vives. A spinner-integrated wind lidar for enhanced wind turbine control. *Wind Energy*, 16:625–643, 2013.
- [15] T. G. Herges, D. C. Maniaci, B. T. Naughton, T. Mikkelsen, and M. Sjöholm. High resolution wind turbine wake measurements with a scanning lidar. *Journal of Physics: Conference Series*, 854:012021, May 2017.
- [16] Atmosphere to Electrons (A2e). Maintained by A2e Data Archive and Portal for U.S. Department of Energy, Office of Energy Efficiency and Renewable Energy, 2016. <https://a2e.energy.gov/projects/wake>.

Acknowledgments

This work was authored [in part] by the National Renewable Energy Laboratory, operated by Alliance for Sustainable Energy, LLC, for the U.S. Department of Energy (DOE) under Contract No. DE-AC36-08GO28308. Funding provided by the U.S. Department of Energy Office of Energy Efficiency and Renewable Energy Wind Energy Technologies Office. The views expressed in the article do not necessarily represent the views of the DOE or the U.S. Government. The U.S. Government retains and the publisher, by accepting the article for publication, acknowledges that the U.S. Government retains a nonexclusive, paid-up, irrevocable, worldwide license to publish or reproduce the published form of this work, or allow others to do so, for U.S. Government purposes. Sandia National Laboratories is a multimission laboratory managed and operated by National Technology & Engineering Solutions of Sandia, LLC, a wholly owned subsidiary of Honeywell International Inc., for the U.S. Department of Energy’s National Nuclear Security Administration under contract DE-NA0003525.

Glossary

U_{hub} Mean hub-height wind speed.

TI_{hub} Hub-height turbulence intensity (two-dimensional) $\sigma_{U_{hub}}/U_{hub}$.

α Exponent of the power-law fit to vertical profile of wind speed between 10 m and 58 m.

z/L Stability parameter (sensor measurement height divided by Obukhov length).

v_{los} Wind velocity along laser line of sight.

u_* Friction velocity.

$\overline{w'\theta'_v}$ Kinematic heat flux at $z = 2$ m.

θ_v Virtual potential temperature at $z = 2$ m.